A comparison of APD and SPAD based receivers for visible light communications

Long Zhang, Danial Chitnis, Hyunchae Chun, Sujan Rajbhandari, *Member IEEE,* Grahame Faulkner, Dominic O'Brien, *Member IEEE,* and Steve Collins, *Member IEEE.*

***Abstract*— Visible light communications (VLC) is an alternative method of indoor wireless communications that requires sensitive receivers. Ideally, single photon avalanche detectors (SPADs) could be used to create more sensitive receivers. However, the dead-time, finite output pulse width and photon detection efficiency of existing SPAD arrays limits their sensitivity and bandwidth. In this paper an accurate equation for the impact of dead-time on the sensitivity of a SPAD array is presented. In addition the impact of the width of the output pulses on the on-off keying (OOK) data rate is investigated. Finally, a comparison between receivers containing an APD and a large array of SPADs shows that although the receiver containing the SPAD is more sensitive in the dark the APD-based receiver is more sensitive in normal operating condition. However, the models that predict the performance of both receivers suggest that newer SPAD arrays will enable significant improvements in receiver sensitivity.**

***Index Terms*—** SPAD, APD, VLC, SPAD-based receivers, Visible light communication, optical wireless communication

I. INTRODUCTION

Optical wireless communications (OWC) has been proposed as an alternative method of indoor wireless communications, which avoids the problems that can occur when using radio-frequency (RF) communications [1,2]. The maximum rate at which data can be transmitted through any channel is determined by the bandwidth and signal-to-noise ratio (SNR) of the channel.

A key component of all OWC systems [3,4,5,6] is the photodetector in the receiver, and, in order to maximise the SNR, some systems use a receiver based upon an avalanche photodiode (APD). In these devices, avalanche multiplication amplifies the signal. Unfortunately, it also generates excess noise that limits the maximum useful APD gain. The impact of this excess noise can be avoided by operating the APD at higher voltages to create a single photon avalanche detector (SPAD) [7,8]. Results obtained using optical receivers that incorporate SPADs have been recently reported [9-13].

Since SPADs can detect single photons, particularly when operated in the wavelength range where they are most sensitive, they potentially have a higher sensitivity than APDs [9]. Existing SPADs, that are manufactured using complementary metal-oxide semiconductor (CMOS) processes, are typically most sensitive at visible wavelengths. Consequently, it is anticipated that a SPAD-based visible light communication (VLC) receiver will support a particular bit error rate (BER) with a lower received optical power in the visible band than an APD-based receiver.

Although SPADs are potentially more sensitive than APDs, they currently have smaller active areas and can have low fill-factors when fabricated in arrays. Additionally, they are blinded for a short time (known as the dead-time), after a photon is detected. When combined with their high sensitivity, this dead-time makes them potentially susceptible to ambient light. The potential impact of ambient light means that, although SPADs have been used in other environments [14-18], it is not obvious that they should be preferred to APDs in the presence of ambient light. In this paper, the first attempt to determine when SPADs should be preferred to APDs is reported. In addition, the potential benefits of using SPADs, rather than APDs, in the presence of ambient light are quantified.

Section II introduces a small array of SPADs with a variable dead-time and presents an analysis of the effect of dead-time on the response of any array of SPADs. Sections III and IV then contain results from experiments on links, including this small SPAD array and an APD receiver respectively. To determine the performance of receivers containing larger arrays of SPADs, the results of experiments on a commercial off-the-shelf array of SPADs are presented in section V. Finally, conclusions are drawn in section VI.

II. THE SPAD ARRAY

A SPAD is created by biasing a photodiode above its breakdown voltage. When operated in this mode, an avalanche event initiated by a photon will become self-sustained and is easily detected. Then, to detect a second photon, this self-sustained avalanche process has to be quenched. A load device is therefore added in series with the photodiode. Whenever an avalanche event occurs and a large current flows through the load, the otherwise self-sustained event is quenched by the resulting reduction in the bias voltage across the photodiode. It takes a finite time for the bias voltage to recover from this quenching process. Hence, each avalanche event is followed by a period, known as the dead-time, during which the SPAD is insensitive to light. The impact of the dead-time can be mitigated by using arrays of SPADs[7,8]. In these arrays, the illuminating photons are spread across the array, so that some

L.Zhang, H. Chun, G. E. Faulkner, D. C. O'Brien and S.Collins are with the Department of Engineering Science, University of Oxford, Oxford, UK. e-mail:{long.zhang, hyunchae.chun, grahame.faulkner, dominic.obrien, steve.collins}@eng.ox.ac.uk.

D. Chitnis is now with School of Engineering, Scottish Microelectronics Centre, The University of Edinburgh, Edinburgh, UK. e-mail: d.chitnis@ed.ac.uk

S. Rajbhandari is now with the School of Computing, Electronics and Mathematics, Coventry University, Coventry, UK. e-mail: sujan.rajbhandari@coventry.ac.uk

SPADs are always active and therefore available to detect incident light.

The impact of dead-time on the performance of SPAD arrays can be determined by comparing the dead-time of a SPAD to the average time between detected photons. For a SPAD with an active area, A_{SPAD}, the average time between detected photons is

$$t_{interdetected} = \frac{E_p}{\eta . A_{SPAD} . (L_{dark} + L)} \quad (1)$$

where L is the intensity of illuminating light in Watts per unit area. L_{dark} is the equivalent intensity that represents the effect of unavoidable dark counts (which occur without any illumination), η is the SPAD photon detection probability (PDP) and E_p is the energy of each photon.

If the light intensity is low enough for $t_{\text{interdetected}}$ to be much longer than the dead-time, then the average number of counts for N_{SPADS} SPADs in an array in a time T will be

$$counts = N_{SPADS} . (L_{dark} + L) . T . \frac{\eta . A_{SPAD}}{E_p} \quad (2)$$

This equation shows that, if the dead-time of the SPADs is orders of magnitude shorter than the time between counts per SPAD, the number of counts is proportional to the illumination intensity. In contrast, at high light intensities, photons will impinge on SPADs that are inactive and the dead-time will reduce the number of counts. At extremely high light intensities, a photon will be detected as soon as the dead-time from the previous detected photon ends. This means that, for an array of SPADs with a dead-time of τ, the maximum number of counts in a time T will be

$$counts_{max} = \frac{N_{SPADS} . T}{\tau} \quad (3)$$

The expected linear response at low-light light intensities and saturation at high light intensities can be obtained using the function

$$counts = \frac{N_{SPADS} . \alpha . T . (L_{dark} + L)}{1 + \alpha . \tau . (L_{dark} + L)} \quad (4)$$

to calculate the number of counts in a time T from an arrays of N_{SPADS}, where for convenience

$$\alpha = \frac{\eta . A_{SPAD}}{E_p} \quad (5)$$

Equation (4) is similar to the equation that has been used to determine the true count rate from the measured count rate for an actively quenched SPAD [19]. However, (4) included a term that takes into account the existence of dark counts.

Table I: Summary of key parameters of the SPAD array.

Process	180nm
Number of SPADs	60
Breakdown Voltage	10.4V
Diameter of Active Area	10μm
Fill Factor	3.2%
Minimum Dead-time	5 ns
Average Dark Count Rate	90kHz
Photon Detection Probability at 650nm with an excess voltage of 1.6V	6.9%

An array of 60 SPADs, whose parameters are listed in Table I, and which is described in more detail in [8], was used to determine the accuracy of (4). In this array, the output from each SPAD is a current. This current is generated using a pair of transistors to steer the current from a constant current source to a common output whenever a photon has been detected. The current is steered to the common output during the SPADs dead-time and the output currents are summed to create a single output. This output is then converted to a voltage using a 50Ω load resistor[8]. Critically for these experiments, the dead-time of the SPADs can be varied using a user controlled input voltage.

Fig 1 shows the average number of counts in a predetermined time against the product of the light intensity and dead-time. This data was obtained by varying both the intensity of light illuminating the SPAD array from a 650 nm Resonant Cavity Light-Emitting Diodes (RCLED) and the SPAD dead-time. In this figure, all the measured data falls on the same curve when the x-axis is dead-time τ multiplied by light intensity L. This occurs because the average number of detected photons depends on the ratio of dead-time and inter-photon time. For a fixed dead-time, decreasing the inter-photon time increases the probability of photons hitting an inactive SPAD, resulting in a higher probability of photons being undetected. Similarly, for a particular inter-photon time, increasing the dead-time will also increase the probability of photons hitting an inactive SPAD. Since the average inter-photon time is inversely proportional to the light intensity, L, the ratio of dead-time to inter-photon time is proportional to the product of dead-time τ and light intensity.

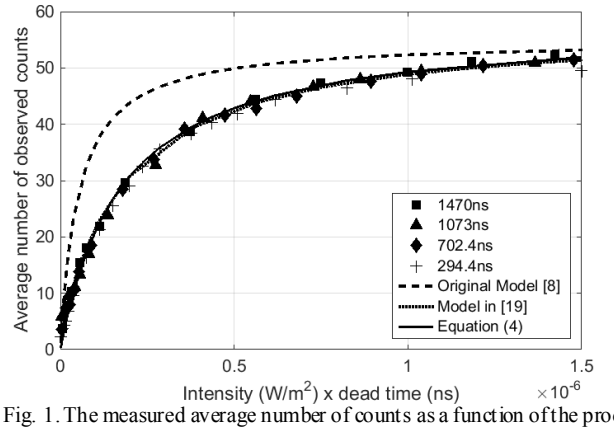

Fig. 1. The measured average number of counts as a function of the product of the intensity of the light falling on the SPAD array and the SPAD dead-time for four different dead-times. This data is compared to the results predicted using (4) and two previously proposed method of determining the impact of dead-time of the performance of an array of SPADs.

Fig 1 also shows the expected number of counts under different conditions obtained using (4). For comparison, the results obtained using two previously proposed methods of the impact of dead-time[8,19] are also shown. Adapting to the notation of this paper, one of these models [8] is

$$counts_{array} = \frac{counts . N_{SPADS}}{N_{SPADS} - counts} \quad (6)$$

where *counts* is calculated using (2). The results in Fig 1 show that this is not an accurate model. The second model [19] is the same as (4) if L_{dark}=0 and, since the dark count rate (DCR) of the tested SPADs is so small, the results from (4) and this model are very similar. A comparison of the data and these two

models shows that, for this SPAD array, both these models accurately predict the response of the array.

The nonlinear response due to the SPAD's dead-time is effectively a reduction in the sensitivity of the SPAD array. The effect of this reduction in sensitivity on data link performance is investigated in the next section.

III. Link Results for the Small SPAD Array

A. BER

The SPAD array was used as the receiver in an optical link. The source in this link was a 650nm RCLED, driven by an HP1130A pattern generator so that it transmitted an OOK modulated pseudorandom binary sequence (PRBS). These experiments were performed with the laboratory lights switched off. However, an optical band-pass filter, with a centre wavelength of 650nm and a 40nm bandwidth, was used to reduce the amount of ambient light from the laboratory equipment that reached the receiver. The output signal from the SPAD array was then captured using a ZS1500 active probe and a HDO6014-MS oscilloscope.

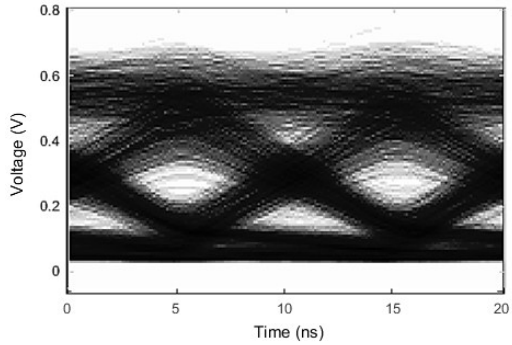

Fig. 2. A raw eye-diagram at a data rate of 100Mbps when the BER is 7.9×10^{-4}.

Fig 2 shows a raw eye-diagram from the oscilloscope when data was transmitted at 100Mbps. For this experiment, a signal light intensity of 1.1 Wm^{-2} was incident on the SPAD array, corresponding to -53dBm incident on the active areas of the device. A notable feature of this eye-diagram is its symmetry. This symmetry arises because the temporal response of the output is determined by the pair of transistors used to control the output current. These two transistors set a threshold voltage and they have identical responses when the SPAD bias voltage increases or decreases through this threshold. It is therefore these transistors that generate the symmetry in the eye-diagram.

A BER of 7.9×10^{-4} was estimated by processing this eye diagram. This BER is below the level at which a standard Forward Error Correction (FEC) code can operate[20], and for convenience this BER was adopted as the reference level for later experiments reported in the paper. It can be seen that the noise is highly signal dependent, with much greater noise occurring when a 1 is being transmitted. This is due to the photon shot noise, which is a significant, if not the dominant, noise source.

B. Effect of dead-time

This type of SPAD array steers the output current associated with each SPAD to the common output during the SPAD's dead-time. This means that the width of the output pulses from this array of SPADs equals the dead-time. If the dead-time, and hence the output pulse width, is much shorter than the bit-time, the responses to photons detected in each bit will not necessarily be added together at the output. In contrast, using a dead-time, and hence output pulse width, that is longer than the bit-time will cause inter-symbol interference (ISI). These two effects lead to the conclusion that the lowest BER will be achieved when the bit-time is approximately equal to the dead-time, and hence output pulse width. Fig 3 shows the measured BER for three different data rates at various dead-times. As expected, these results show that the best BER for a particular data rate is achieved when the dead-time of this type of SPAD array is slightly shorter than the bit-time for the data rate.

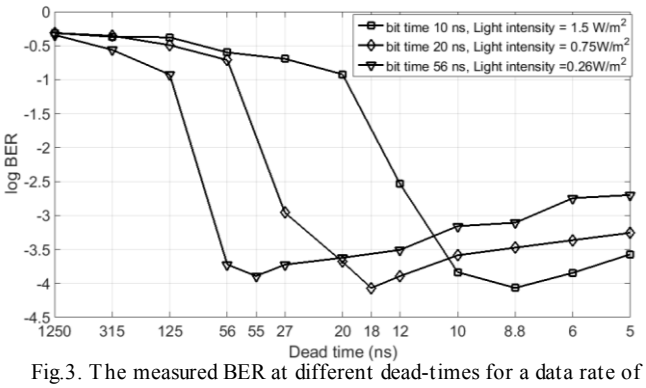

Fig.3. The measured BER at different dead-times for a data rate of 100 Mbps, 50 Mbps and 17.9 Mbps. In each case the lowest BER is achieved for a dead time which is slightly shorter than the bit time.

C. Probability density function (PDF) of received data.

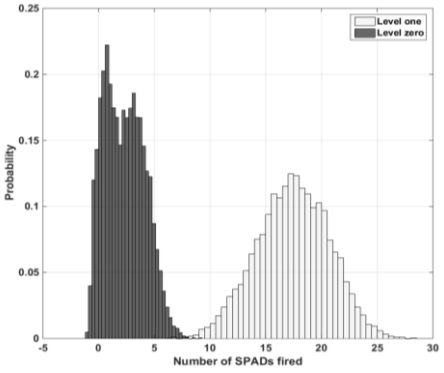

Fig.4. The measured histograms of the number of SPADs that have fired within a dead-time of the end of each bit period when the bit-time is 10 ns, the dead-time is 8.8 ns and the measured BER is 7.9×10^{-4}.

Fig 4 shows the histogram of number of SPADs that are contributing to the output voltage at the instant when the SPAD output is converted into a bit stream. This variable equals the effective number of detected photons per bit that are required to achieve a BER of 7.9×10^{-4}. The results show that the number of photons detected when a zero is transmitted is a bimodal distribution. The lower peak is the 'true' zero PDF, set by the electronic noise of the system with no received photons (approximately 72mVpp). In addition, ISI causes a secondary peak with a maximum voltage that corresponds to approximately 3 detected photons per bit. When a "1" is transmitted, the mean increases and the shot noise from the additional photons causes a broader peak. These results show that, with this SPAD array,

a BER of 7.9×10^{-4} can be achieved using approximately 15 detected photons per bit. Decision feedback equalisation (DFE) can be used to reduce the impact of ISI [21,22]. In these experiments, the least mean square (LMS) algorithm was used to find the optimum coefficients for a DFE equaliser. When this equalization is used, a 3dB improvement in receiver sensitivity can be achieved (corresponding to an average of 10.2 detected photons per bit).

For these experiments, the SPAD array was tested in the dark and a significant component of the noise when a 0 is transmitted is electronic noise rather than Poisson noise. However, in the presence of ambient light, Poisson noise is expected to dominate. For a system limited by Poisson noise, the BER can be estimated using

$$BER = \frac{1}{2}\sum_{k=0}^{n_T}\frac{(N_1)^k}{k!}e^{-N_1} + \frac{1}{2}\sum_{k=n_T}^{\infty}\frac{(N_0)^k}{k!}e^{-N_0} \qquad (7)$$

where N_0 is the number of counts detected for a zero, N_1 is the number of detected counts when a one is transmitted and n_T is the decision threshold. In the absence of ambient light, the number of counts detected when a "0" is being transmitted is ideally zero. Under these conditions, (7) can be used to show that, for a system limited by Poisson noise, a BER of 7.9×10^{-4} can be achieved with an average of 6.5 detected photons per bit. In fact the SPAD array only requires an average of 10.2 detected photons per bit to achieve this BER. When detected photons per bit are considered, the performance of the SPAD array is close to that of an ideal receiver (RX) that is limited by Poisson noise.

D. Effect of ambient light.

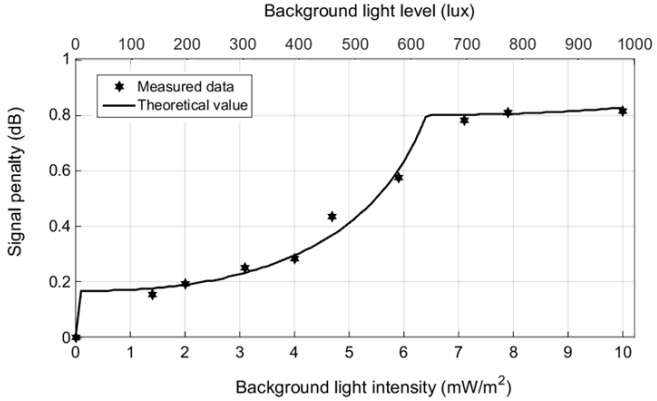

Fig. 5. The signal penalty required for the SPAD to achieve a BER of 7.9×10^{-4} at different background light levels, shown in both mW/m^2 (bottom x-axis) and lux (top x-axis), for 100Mbps when equalization has been used to reduce ISI.

The link described in Section III.A was operated in the absence of ambient light. When a VLC system is operated in offices or homes, it will be impossible to always exclude ambient light. The link was therefore operated under normal levels of room lighting after an aperture had been added to the receiver described in Section III.A. This aperture was used to restrict the FOV of the detector to approximately 24 degrees. This reduces the ambient light reaching the SPAD array, whilst maintaining a practical FOV. The amount of ambient light reaching the SPAD was then varied by dimming the room's fluorescent lighting.

Fig 5 shows the additional signal intensity required to achieve a BER of 7.9×10^{-4}, after equalization (EQ), at 100 Mbps for different background light levels. Fig 5 also includes a line that represents the additional signal intensity required to achieve this BER calculated using (7). The most notable feature of the results obtained from (7) is the change in these results at approximately 6.5 mW m^{-2}. This feature arises because the decision threshold in (7) is an integer. In particular, as the background light intensity increases from 1 mW m^{-2} to 6.5 mW m^{-2}, the probability of a transmitted "0" being misinterpreted as a "1" increases. In order to achieve the target BER, the signal level has to increase so that the probability of a "1" being misinterpreted as a "0" is reduced. However, once all the allowed errors are caused by "0"s being misinterpreted as "1"s, the decision threshold has to increase. Once this occurs almost all the errors are "1"s being interpreted as "0"s. As the background light intensity increases further, again the signal intensity has to increase to maintain the BER. Eventually the threshold has to change again and a feature similar to the one at 6.5 mW m^{-2} will occur at a higher background light level.

The excellent agreement between the measured data and the results of (7) confirms that, in ambient light, the dominant noise source in the SPAD array is Poisson noise. Furthermore, these results show that, with straightforward precautions, links containing SPAD arrays only require modest increases in transmitted power to operate in realistic ambient light conditions.

IV. LINK RESULTS FOR AN APD RECEIVER

To allow a comparison with the small SPAD array, the sensitivity of an AD1900-9-TO5i APD (3mm^2 active area) and a MAX3665 transimpedance amplifier with a bandwidth of 90MHz, has also been measured. When the APD was operated at its measured optimum bias (150V), -50dBm (corresponding to 3.44mW m^{-2} at the receiver) is required to achieve the reference BER of 7.9×10^{-4} at 100Mbps in the dark.

When ambient light reaches the APD, the additional shot noise means that a higher signal power will be required to maintain the same SNR and hence BER. If the dominant noise source in a receiver is assumed to have a Gaussian distribution, the BER can be calculated using [21]

$$BER = 0.5.erfc\left(\frac{Q}{\sqrt{2}}\right) \qquad (8)$$

where Q is the signal to noise ratio. For an APD, Q is

$$Q = \frac{m.R.P_s}{\sqrt{2e.(R.(P_b+P_s)+I_d).bw.m^{x+2}+i_{th}^2}+\sqrt{2e.(R.P_b+I_d).bw.m^{x+2}+i_{th}^2}} \qquad (9)$$

where m is the APD gain, R is the APD responsivity, P_s is the signal light power, P_b is the background light power, I_d is the dark current, x is the excess noise index, bw is the bandwidth and i_{th}^2 is the thermal noise of the detector.

The denominator of (9) shows that the noise in the APD increases when the background light power increases. The effect of ambient light on the link containing the APD was measured using the same experimental procedure used to measure the effect of ambient light on the SPAD array. The measured signal penalties required at different ambient levels are shown Fig 6. This figure also shows the theoretical signal penalty required to obtain a BER of 7.9×10^{-4} calculated using (9) and the parameters in Table II. The results in this figure

show that (9) and the parameters in Table II can be used to accurately determine the increase in transmitted power needed to maintain a target BER in the presence of ambient light.

Table II: Summary of parameters used to calculate the SNR of the APD.

Characteristics	Value
Active area	3 mm^2
Dark current @ m=100	15nA
Responsivity @ m=100 and λ= 650nm	35 AW^{-1}
APD gain @ 150V	105
Excess noise index	0.36
Target BER	7.9×10^{-4}
Data rate	100Mbps

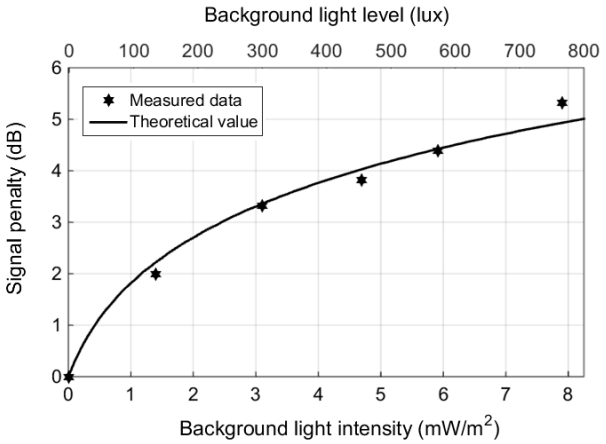

Fig.6. The required signal penalty for the APD to achieve a BER of 7.9×10^{-4} at various background light intensities. In this figure the data (stars) is compared to the predictions of (9).

V. LINK RESULTS WITH A LARGE ARRAY OF SPADS

The signal intensities required to achieve the target BER show that the APD receiver is approximately 22dBs more sensitive than the small SPAD array. However, the active area of the APD is approximately 640 times larger than the active area of the SPAD array but the SPAD array only requires 161 times the light intensity of the APD. This suggests that larger arrays of SPADs could be used to create more sensitive receivers than APDs.

A larger array of the SPADs described in section II could be manufactured and tested. This would give an opportunity to increase the sensitivity of the SPAD array by increasing its fill-factor, and hence photon detection efficiency (PDE). Unfortunately, any increase in fill-factor would be associated with a reduction in the number of SPADs per unit area. An optimum design for a SPAD array would therefore be based upon information about the minimum PDE needed for a SPAD-based receiver to match the sensitivity of an APD-based receiver.

Large SPAD arrays can be purchased that are designed for photon counting. These arrays are not optimised for VLC, however, the performance of receivers containing a larger number of SPADs has been investigated using a C11209-110 optical measurement module. The light sensitive part of this commercial off-the-shelf module is an array of SPADs, or multi-pixel photon counter (MPPC). The photodetector has a photosensitive area of 1 mm by 1 mm, containing 10,000 individual SPADs with a 10 µm pitch and a fill-factor of 33%. With an applied voltage of 5 V the measured PDP of this MPPC was 24% at 650 nm, which means that at this wavelength the PDE of this device is 8%.

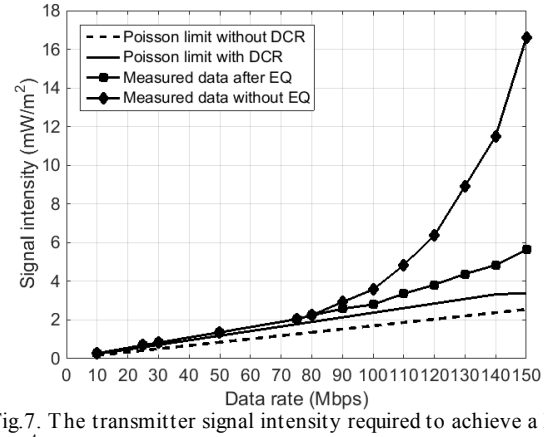

Fig.7. The transmitter signal intensity required to achieve a BER of 7.9×10^{-4} at different data rates when the MPPC is used as the receiver. This measured data is compared to results obtained from (7) with and without the SPADs dark counts.

At low light levels, the output from the module consists of discrete pulses and, since each pulse corresponds to a detected photon, the number of detected photons can be counted by counting output pulses. However, at higher light levels, the pulses overlap. Once this occurs, the manufacturer suggests that the output signal from the module should be treated as an analogue signal and low-pass filtered. When the module is used as a receiver, pulse counting gives the best BER for light intensities less than 1.4 $mW\,m^{-2}$. The target BER this light intensity corresponds to a data rate of 25 Mbps. For higher data rates, lower BERs were obtained when the module output was low-pass filtered with the cut-off frequency equal to the data rate.

The measured signal intensities at the receiver needed to achieve the target BER of 7.9×10^{-4} at different data rates, in the dark, are shown in Fig 7. These results show that once the bit time becomes comparable to 10 ns, which is the characteristic time of each output pulse, the transmitted signal intensity required to achieve the target BER increases rapidly. However, using DFE to reduce inter-symbol interference (ISI) significantly reduces the required signal intensity. Consequently, when DFE is employed, the receiver needs 1.64 times more transmitted power to achieve the target BER at 100 Mbps than expected when a receiver is working at the Poisson limit. However, the two sets of results calculated using (7), and included in Fig. 7, show that more than half of this increase in power is required to overcome the SPADs dark count rate. When this effect is included, the receiver only needs 1.17 times more transmitted power than calculated using (7).

Despite these power penalties and a PDE of 8%, the SPAD-based receiver achieves a BER of 7.9×10^{-4} at 100 Mbps with only 80% of the transmitted optical power required by the APD-based receiver. This means that, in the absence of ambient light, these larger SPAD arrays can be used to make receivers that are more sensitive than the receivers containing an APD.

Again the effect of ambient light on the link performance was measured using the experimental procedure used with the

other two receivers. The measured signal penalties required at different ambient levels are shown Fig 8. This figure also shows the theoretical signal penalty required to obtain a BER of 7.9×10^{-4} in the presence of shot noise created by the ambient light. The results in this figure show that (7) can be used to calculate the additional power needed to transmit data and achieve the target BER in the presence of ambient light. This means that shot noise from ambient light explains the additional power needed to transmit data in ambient light. Since shot noise is the only noise source for the SPAD-based receiver, whilst the APD-based receiver also suffers from excess shot noise and thermal noise in the electronics associated with the APD, the SPAD-based receiver requires more additional transmitted power to operate in ambient light.

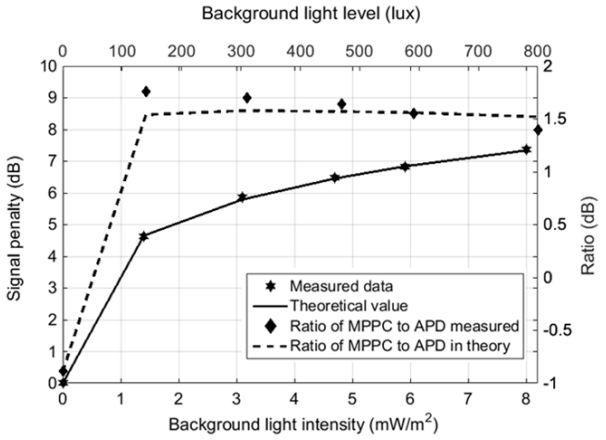

Fig. 8. The required signal penalty for the MPPC to achieve a BER of 7.9×10^{-4} at various background light intensities. In this figure the data (stars) is compared to the predictions of (7)

The ratio between the powers needed to transmit data to the receiver containing the APD and to the receiver containing the MPPC is also shown in Fig. 8. These results show that, although the MPPC-based receiver is more sensitive than the APD-based receiver in the dark, the APD-based receiver is more sensitive in ambient light.

The results in Figures 6 and 8 show that the behaviour of the two types of receivers can be predicted using either (7) or (8) and (9). These equations have therefore been used to determine the signal intensity that is expected to give the target BER at different background light intensities. The results in Fig. 9 show that a receiver containing an MPPC with a PDE of 8% and a power penalty of 1.17 is expected to require more transmitter power than the APD-based receiver at background light intensities of more than 30 $\mu W\,m^{-2}$. Consequently, when the ambient light level is 500 lux, the MPPC requires 1.45 times more transmitted signal than the APD to achieve the target BER.

The MPPC that has been used in these experiments has a PDE of only 8%. However, since SPADs are a relatively new technology, new products have significantly better characteristics than their predecessors. The PDE that is required for an MPPC to match the performance of an APD can be estimated by comparing the SNRs of the two devices under the same conditions. In particular, since shot noise dominates in the APD in ambient light, the SNRs of a SPAD-based receiver and an APD-based receiver at the same transmitter and ambient light intensities is

$$\frac{SNR_{SPAD}}{SNR_{APD}} = \sqrt{\frac{m^x.PDE(\lambda)}{QE(\lambda).PP}} \tag{10}$$

where m, x and $QE(\lambda)$ are the gain, excess noise factor and quantum efficiency of the APD, $PDE(\lambda)$ is the photon detection efficiency of the MPPC and PP is the MPPC's power penalty. This is the ratio between the transmitted power needed by the real SPAD-based receiver and the transmitted power needed by an ideal, shot noise limited receiver. In ambient light, the dark count rate is insignificant compared to the count rate from the ambient light. The relevant power penalty for the tested MPPC is therefore 1.17.

For the APD tested in this paper x is 0.36 and the measured optimum gain is 105, hence m^x=5.3. At 650nm the quantum efficiency of the APD is approximately 65%. Equation (10) therefore suggests that an ideal SPAD array will need a PDE of 14.3% to match the SNR of this APD when shot noise is the dominant noise source. The results in Fig. 9 confirm that (10) gives an accurate estimate of the MPPC PDE that matches the performance of the APD.

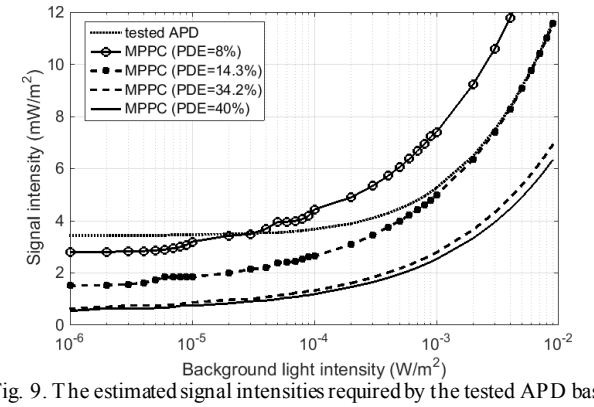

Fig. 9. The estimated signal intensities required by the tested APD based receiver and receivers including MPPCs with different PDEs to achieve the target BER at different intensities of background light.

Unfortunately, the maximum PDE of the MPPC integrated into the C11209-110 that was used in these experiments is less than 14%. However, MPPCs have just become available with PDEs that are significantly higher than 14%. In particular, the recently released S12572-015C has the same output pulse width, and hence bandwidth as the tested MPPC; a comparable dark count rate and a maximum PDE of 40%. In addition, because less than 40 detected photons per bit will be required to transmit data using OOK, the 40,000 individual SPADs in this detector will mean that it will not be affected by the non-linearity observed in Fig. 1.

The performance of an MPPC with a PDE of 40% has been simulated and the results of this simulation have been included in Fig. 9. These results suggest that, under typical ambient lighting conditions, the APD is expected to require between 1.8 and 2.1 times higher signal intensity than this new MPPC. However, these new devices may also require more transmitted power than an ideal receiver. Fig. 9 therefore also includes simulation results for an MPPC with a PDE of 34.2%, which corresponds to a PDE of 40% and a power penalty of 1.17. In this case, under typical ambient lighting conditions, a receiver containing the new MPPC is expected to be between 1.7 and 1.9 more sensitive than a receiver containing an APD.

VI. CONCLUSIONS

SPAD photodetectors produce an output pulse for each detected photon but their sensitivity can be reduced by their dead-time and a low fill-factor. In this paper an expression for the impact of dead-time on the linearity of the response of an array of SPADs has been derived and shown to agree with results obtained with an array of SPADs with a variable dead-time. Results from this small array also show that if operated at data rates where the bit time is longer than the output pulse width, then almost Poisson limited performance can be achieved. Consequently, this receiver requires approximately 45 times fewer detected photon per bit than a state-of-the-art APD. Such an improvement is extremely valuable. However, the experimental SPAD array was too small to be used to create a receiver that can compete with an APD-based receiver.

Results from experiments with a larger SPAD array have also been presented. These results show that, when this large SPAD array is used as a receiver, the transmitted power needed to obtain a target data rate increases rapidly once the bit time becomes shorter than the width of the array's output pulses. The maximum OOK date rate at which this receiver can operate efficiently is therefore limited by the width of the output pulses.

Results have also been presented which show that the SPAD array is more sensitive to ambient light than the APD. Consequently, the receiver containing the APD is a more sensitive receiver in typical ambient light conditions. This situation arises because the particular SPAD array used in the experiments has a PDE of only 8%.

Unlike APDs, SPADs are a relatively new technology and so new products are becoming available that have significantly better characteristics than their predecessors. Expressions for the SNRs of SPAD arrays and APDs have therefore been used to show that a receiver containing a SPAD array with a PDE of 14% would match the sensitivity of the APD-based receiver. . Furthermore, simulation results show that a receiver containing a recently released SPAD array with a maximum PDE of 40% is expected to be significantly more sensitive than an APD-based receiver.

In the future, the simplest way to increase the PDE of SPADs further will be to increase the area of each SPAD in an array. However, this will reduce the number of SPADs per unit area and this will be associated with a loss in sensitivity arising from the effect of dead-time. The optimum receiver sensitivity will therefore be achieved by using the equations in this paper to increase the PDE of each SPAD whilst limiting detrimental dead-time effects. The anticipated results will be additional increases in receiver sensitivity.

REFERENCE

[1] H. Haas, L. Yin, Y. Wang and C.Chen, "What is LiFi?," *J. Light. Technol*, vol. 34, no. 6, pp. 1533–1544,2016.

[2] T. Komine and M. Nakagawa "Fundamental analysis for visible light communication system using LED lights.," *IEEE Trans. Consum. Electron.*, vol. 50, no. 1, pp. 100–107, 2004.

[3] J. M. Kahn and J. R. Barry, "Wireless Infrared Communications," *Proc. IEEE,* vol.9219, no. 97, 1997.

[4] D. Tsonev, H. Chun, S. Rajbhandari, J. J. D. McKendry, S. Videv, E. Gu, M. Haji, S. Watson, A. E. Kelly, G. Faulkner, M. D. Dawson, H. Haas, and D. O'Brien, "A 3-Gb/s single-LED OFDM-based wireless VLC link using a gallium nitride microLED," *IEEE Photonics Technol. Lett.*, vol.26, no. 7, pp. 637–640, 2014.

[5] A. H. Azhar, T. Tran, and D. O'Brien, "A Gigabit/s Indoor Wireless Transmission Using MIMO-OFDM Visible-Light Communications," *IEEE Photonics Technol. Lett.*, vol. 25, no. 2, pp. 171–174, 2013.

[6] F. M. Wu, C. T. Lin, C. C. Wei, C. W. Chen, Z. Y. Chen, H. T. Huang, and Sien Chi, "Performance Comparison of OFDM Signal and CAP Signal Over High Capacity RGB-LED-Based WDM Visible Light Communication," *IEEE Photonics J.*, vol. 5, no. 4, pp. 7901507–7901507, 2013.

[7] E. Fisher, I. Underwood, and R. Henderson, "A reconfigurable 14-bit 60Gphoton/s Single-Photon receiver for visible light communications," *Eur. Solid-State Circuits Conf.*, pp. 85–88, 2012.

[8] D. Chitnis and S. Collins, "A SPAD-based photon detecting system for optical communications," *J. Light. Technol.*, vol. 32, no. 10, pp. 2028–2034, 2014.

[9] Y. Li, M. Safari, R. Henderson, and H. Haas, "Optical OFDM With Single-Photon Avalanche Diode," *IEEE Photonics Technol. Lett.*, vol. 27, no. 9, pp. 943–946, 2015.

[10] S. Gnecchi, N. A. W. Dutton, L. Parmesan, B. R. Rae, S. Pellegrini, S. J. Mcleod, L. A. Grant, and R. K. Henderson, "Analysis of Photon Detection Efficiency and Dynamic Range in SPAD-Based Visible Light Receivers," *J. Light. Technol*, vol. 34, no. 11, pp. 2774–2781, 2016.

[11] E. Fisher, I. Underwood, and R. Henderson, "A reconfigurable single-photon-counting integrating receiver for optical communications," *IEEE J. Solid-State Circuits*, vol. 48, no. 7, pp. 1638–1650, 2013.

[12] O. Almer, D. Tsonev, N. A. W. Dutton, T. Al Abbas, S. Videv, S. Gnecchi, H. Haas, and R. K. Henderson, "A SPAD-based Visible Light Communications Receiver Employing Higher Order Modulation," *IEEE Global Telecommun.Conf*, 2015.

[13] D. Chitnis, L. Zhang, H. Chun, S. Rajbhandari, G. Faulkner, D. O'Brien, and S. Collins, "A 200 Mb / s VLC demonstration with a SPAD based receiver," in *IEEE SUM*, 2015,vol.3,pp. 226-227.

[14] Y. Li, S. Videv, M. Abdallah, K. Qaraqe, M. Uysal, and H. Haas, "Single photon avalanche diode (SPAD) VLC system and application to downhole monitoring," in Proc. *IEEE Global Commun. Conf.*, 2014.

[15] Y. Li, M. Safari, R. Henderson, H.Haas, "Nonlinear Distortion in SPAD-Based Optical OFDM Systems", *IEEE*, *Globecom Workshops 2015,* pp. 1-6.

[16] M.A.Khalighi, T.Hamza, S. Bourennane, P. Léon, J.Opderbecke, "Underwater Wireless Optical Communications Using Silicon Photo-Multipliers", *IEEE Photonics J.*, vol. 9, pp. 1-10, 2017.

[17] T. Shafique, O. Amin, M. Abdallah, I. S. Ansari, M.S Alouini, K. Qaraqe, "Performance Analysis of Single-Photon Avalanche Diode Underwater VLC System Using ARQ", *IEEE Photonics J.*, vol. 9, pp. 1-11, 2017.

[18] C.Wang, H.Y. Yu, Y.J. Zhu, and T. Wang, "Blind Detection for SPAD-based Underwater VLC System under Poisson-Gaussian Mixed Noise Model", *IEEE Commun. Lett*, 2017.

[19] A. Eisele, R. Henderson, B. Schmidtke, T. Funk, L. A. Grant, J. A. Richardson, and W. Freude, "185 MHz Count Rate, 139 dB Dynamic Range Single-Photon Avalanche Diode with Active Quenching Circuit in 130nm CMOS Technology," in. IISW, Japan, 2011, pp. 278–281.

[20] ITU-T,G.975.1:Forward error correction for high bit-rate DWDM submarine systems, 2004.

[21] J. G. Proakis, "Digital Communications," *McGraw-Hill*, 2007.

[22] Govind P.Agrawal, "Fiber Optic Communication Systems," John Wiley & Sons. Inc, 1997.